PREPARATION BY FLAME SPRAY PYROLYSIS OF $ABO_{3\pm\delta}$ CATALYSTS FOR THE FLAMELESS COMBUSTION OF METHANE

Gian Luca Chiarello, Ilenia Rossetti, Paolo Lopinto[a], Gabriele Migliavacca[a] and Lucio Forni*

Dip. di Chimica Fisica ed Elettrochimica, Università degli Studi di Milano

v. C. Golgi, 19 I-20133 Milano, Italy

[a] Stazione Sperimentale per i Combustibili, S.Donato Milanese (MI), Italy

ABSTRACT

Perovskitic mixed oxides prepared through flame-spray pyrolysis possess a good stability in high-temperature application, *viz.* the catalytic flameless combustion of methane. Some preparation operating parameters are here analysed, such as O_2 pressure drop along the spraying nozzle, O_2 discharge velocity and flow rate. These parameters have been correlated with specific surface area, activity and durability of the prepared samples, as well as with flame temperature, varied by using different fuel mixtures. It was found that specific surface area increases with increasing O_2 velocity and flow rate and with decreasing the combustion enthalpy of the solvent mixture. This reflects on both activity and durability of the catalyst.

Keywords: Flame-spray-pyrolysis; Catalytic flameless combustion of methane; Perovskitic mixed oxides.

* Corresponding author: Fax: +39-02-50314300; e-mail: lucio.forni@unimi.it

1 - INTRODUCTION

The catalytic flameless combustion (CFC) of hydrocarbons, particularly of methane, can be carried out at lower temperature (800-900°C) with respect to traditional combustion, so virtually suppressing any NO_x formation. Moreover, the presence of catalyst increases considerably the selectivity to complete oxidation, so eliminating also other hazardous pollutants, such as CO and partial oxidation products.

Perovskitic mixed oxides proved since long time to be valuable substitutes of noble metal based catalysts for the CFC of methane [1-4]. The main properties of a good perovskitic catalyst for CFC are a high ionic mobility through the crystal lattice, a high surface area and mostly a sufficient thermal resistance, hardly obtainable all at once when using traditional preparation methods. Indeed, the perovskitic phase forms at high temperature, usually higher than 700°C. However, under these preparation conditions surface area is usually insufficient for a satisfactory catalytic activity. Hence, special procedures have to be employed for the preparation of active and stable catalysts for the CFC of methane.

Some years ago we developed a flame hydrolysis technique (FH), able to combine high surface area, and hence high catalytic activity, with high thermal stability [3-5]. Indeed, our FH-prepared perovskitic catalysts were characterised by nanometer size particles with high phase purity, relatively high surface area (*ca*. 20 m^2/g) and exceptionally high thermal stability [3-8]. The method was based on nebulising an aqueous solution of the oxide precursors in a H_2+O_2 flame.

Aerosol or liquid-feed flame pyrolysis (FP) are reported to be high temperature synthesis procedures, characterised by productivities generally much higher than that of our FH method [9-15]. Among the methods proposed, the spray FP seems the most

interesting for the production of perovskitic oxides, since it does not require volatile precursors. Hence, the aim of the present work was to set-up a FP apparatus for preparing perovskitic catalysts for the CFC of methane. Attention was paid to the structural homogeneity of the product, particularly important for mixed oxides synthesis. $LaCoO_3$ was chosen as model catalyst, checking how surface area, particle size, phase purity and crystal structure (and hence catalytic performance) are affected when varying some significant preparation operating parameters. Among these, particularly the effect of flow rate and linear velocity of the dispersing-oxidising oxygen and of liquid feed composition on catalyst properties are here analysed.

2 - EXPERIMENTAL

2.1 - Precursors solution

The solutions were prepared by dissolving in propionic acid $La(CH_3COO)_3 \cdot 2H_2O$ (Aldrich, purity > 99.9%) and $Co(CH_3COO)_2 \cdot 4H_2O$ (Merck, purum) in the desired ratio and metal concentration. In some cases different amounts of xylene (Aldrich, thermodynamic equilibrium mixture, purity > 99%) were added to the propionic acid solution.

2.2 – Flame-pyrolysis (FP) apparatus

Our home-made FP apparatus is composed of three sections: *a*) the flame reactor (burner), *b*) the feeding rate control devices for supplying gaseous and liquid reagents and *c*) the catalyst powder collection system.

The burner has been described in detail in [16]. Briefly, it consists of a capillary tube (inner diameter 0.6 mm) ending in the centre of a vertical nozzle and connected with a

syringe pump (Harvard, mod. 975), feeding the solution of the mixed oxide precursors. The nozzle is fed with oxygen (SIAD, purity >99.95%), acting both as oxidant and as dispersing agent, able to form micro-droplets of solution. The main flame is ignited and supported by a ring of twelve premixed O_2 + CH_4 flamelets. Gas flow rate is regulated by MKS (mod. 1259C) mass flow meters, controlled by a MKS (mod. 247 C) control unit. The synthesised nano-particles are collected by means of a 10 kV electrostatic precipitator [5].

High-resolution thermal maps of the flame were recorded through an Agema Thermovision 900 apparatus, equipped with close-up lens and with a data processing unit for real-time image analysis. Conversion of the IR signal to actual temperature values was performed through independent measurements by a 13%Rh-Pt thermocouple, placed inside the flame.

2.3 – Catalyst characterisation

BET specific surface area (SSA) was measured by N_2 adsorption/desorption at 77K on a Micromeritics ASAP 2010 apparatus, after outgassing at 300°C for at least 6 h. Scanning electron microscopy (SEM) analysis was carried out on a LEICA LEO 1430 instrument. A Philips PW1820 powder diffractometer was employed for structural analysis. The diffractograms obtained were compared with literature data for phase recognition [17].

2.4 – Catalytic activity tests

Catalytic activity tests for the CFC of methane were carried out by means of a continuous quartz tubular reactor (i.d.= 7 mm) heated by a tubular furnace through two heavy metal blocks. The catalyst (*ca*. 0.2 g, 0.15-0.25 mm particle size) was placed in the isothermal middle part of the reactor, between two flocks of quartz wool, after dilution with

1.3 g of quartz particles of the same size. The void part of the reactor tube, above and below the catalyst bed, was filled with 10-20 mesh quartz beads. Prior to each run, the catalyst was activated in flowing air (20 cm^3/min), while increasing temperature by 10°C/min up to 600°C, then kept for 1 h. The activity tests were carried out by feeding a mixture composed of 0.5 vol% CH_4, 49.5 vol% He and 50 vol% air, while increasing temperature by 2°C/min from 250 up to 600°C. The outcoming gas was analysed in line by means of a HP 5890 gas chromatograph. The total flow rate of the reactants mixture was calculated by referring to the mass of active phase, so to have for every test an identical value of time factor τ = W/F=10 (mg of perovskite·min/cm^3 of overall gas flow rate).

2.5 - Accelerated thermal deactivation tests

Accelerated thermal deactivation tests were carried out after keeping the sample at the temperature of maximum conversion (T_f, slightly variable from 475 to 500°C, depending on the sample) for 48 h, measuring the residual conversion every 24 h. Then cycles of reaction/deactivation were accomplished by increasing temperature (10°C/min) up to 800°C, kept for 1 h. The temperature was then brought back to T_f, kept for 3 h, during which the catalytic activity was measured. The cycles were repeated for at least three times.

3 – RESULTS AND DISCUSSION

The FP technique is very versatile, depending on many different parameters, sometimes contrasting with each other [16]. Here we took into account only some of the

most critical ones, *i.e*. liquid feed composition, O_2 flow rate and pressure drop along the nozzle.

3.1 – Effect of O_2 linear velocity and flow rate

A previous study on the nozzle aimed at calculating the main working parameters, such as the discharge coefficient and the equivalent discharge cross section, from which it was possible to determine the O_2 linear speed under different working conditions [16].

O_2 linear velocity mainly determines the residence time of the primary particles in the flame. The lower the latter parameter, the lower is particle sintering [18] and hence the higher is the SSA of the produced powder oxide(s). However, a too low residence time into the flame can lead to insufficient thermal resistance of the catalyst. Moreover, the permanence of the precursors into the flame must allow their full conversion into the desired phase, together with the complete elimination of the organic matter (solvent and precursors anions). As a consequence, the shortening of flame height due to the increase of O_2 velocity is one of the main effects on the residence time into the flame, as well as on catalyst thermal resistance [16,18], especially when passing from laminar to turbulent flow regime. However, the deepest effect was observed on particle size distribution. Indeed, with a laminar flow regime a poor size uniformity was obtained. By contrast, under turbulent flow regime a much better size homogeneity was reached, the product consisting of nanospheres with 20 nm mean diameter [16]. A similar behaviour was observed during the preparation of V-Ti oxide through aerosol flame synthesis [19].

The transition from laminar to turbulent flow regime, when increasing pressure drop (Δp) along the nozzle and hence O_2 discharge velocity, has been evidenced by means of the infrared camera imaging (Fig.1). The instantaneous images of the flame, obtained with

Δp=1.5 and 0.3 bar, respectively, are reported in Fig.1*A* and 1*B*. In the first case one may observe the shortening of the flame height and the formation of eddies, absent in Fig.1*B*.

The flame temperature is reported in Table 1, both as absolute maximum temperature, always located at the flamelets crown, and as maximum temperature in the main flame. Concerning the IR measurements at the flamelets crown, one has to consider that temperature values can be overestimated, due to the presence of a solid surface, having different emissivity from that of the gas phase. In any case it may be noticed that, as expected, flame temperature is lower when O_2 speed is higher, *i.e.* when O_2 Δp through the nozzle is higher.

The dependence of powder SSA on O_2 discharge velocity is reported in Fig.2. It can be observed that raising O_2 rate allows to linearly increase SSA. This also entrains a parallel increase of catalytic activity (*vide infra*).

As for thermal resistance under the highly demanding CFC working conditions, it was observed that once a pure perovskitic phase forms, catalyst resistance always increases with decreasing SSA. Hence, from a practical point of view, in order to improve thermal stability one has to increase particle sintering, at the expenses of a slightly lower activity. Nonetheless, the present activity data (*vide infra*) allow to conclude that the FP technique leads in any case to highly active catalysts, which completely convert methane below 500°C, even under the less favourable catalyst preparation conditions.

The dependence of surface area, and hence of particle size, on O_2 flow rate is rather complex. With constant nozzle geometry and at subsonic nozzle discharge rate, an increase of O_2 flow rate entrains an increase of linear velocity. Therefore, an increase of surface area can be surely attributed to the faster travelling of the primary particles through a progressively shorter flame, which prevents any significant particle sintering. However, when increasing O_2 flow rate at constant liquid feeding rate, a higher dispersion of the particles in the flame is obtained, decreasing the probability of collision between them, *i.e*.

limiting particles sintering. Furthermore, an excess of O_2 has also a quenching effect, lowering flame temperature and hence particle sintering [16]. O_2 flow rate is hence a very critical parameter, allowing or not the formation of the desired product, apart from its physical properties. Indeed, when the O_2 flow rate is too high with respect to liquid flow rate, the quenching effect becomes excessive, so inhibiting the formation of the perovskitic phase, due to the too low flame temperature.

3.2 – Effect of solvent nature

Catalyst thermal resistance can be improved by increasing flame temperature. This can be effectively achieved by a proper selection of the solvent mixture. As an example, Fig.3 shows the effect of the addition of xylene to propionic acid on the combustion enthalpy (ΔH_c) of the solvent, here referred to unit volume of liquid fuel mixture and on the SSA of the prepared catalyst. A progressive increase of flame temperature with increasing the amount of xylene, *i.e.* the combustion enthalpy of the fuel (Tab.1 and Fig.1*C*-*E*), can be noticed, accompanied by a decrease of SSA. This reflects only slightly on catalytic activity (Fig.4), but rather heavily on thermal resistance, which improves considerably with increasing the xylene fraction in the fuel (Fig.5).

CONCLUSIONS

The FP synthesis method shows a versatile technique for the continuous, high-yield one-step preparation of perovskitic oxides. For catalytic application at low temperature, activity can be privileged by decreasing particle size, and hence increasing SSA, through proper setting of the preparation parameters. By contrast, when the catalyst has to be employed at high temperature, such as for the CFC of methane, high thermal stability

becomes a must. This can be achieved satisfactorily, either by increasing the flame temperature, or by increasing the residence time of the powder in the hottest zone of the flame, *e.g.* by lowering the oxygen linear velocity through a proper setting of O_2 flow rate and pressure drop along the nozzle, or by increasing the combustion enthalpy of the fuel mixture.

REFERENCES

[1] - J.L.G. Fierro, J.M.D. Tascòn, L.G. Tejuca, J. Catal., 93 (1985) 83.

[2] - R.J.H. Voorhoeve, J.P. Remeika, D.W. Johnson, Science, 180 (1973) 62.

[3] - R. Leanza, I. Rossetti, L. Fabbrini, C. Oliva, L. Forni, Appl. Catal. B: Environ., 28 (2000) 55.

[4] - I. Rossetti, L. Forni, Appl. Catal. B: Environm., 33 (2001) 345.

[5] - R.A.M. Giacomuzzi, M. Portinari, I. Rossetti, L. Forni, in: A. Corma, F.V. Melo, S. Mendioroz, J.L.G. Fierro (Eds.), Study of Surface Science and Catalysis, Vol. 130, Elsevier, Amsterdam, 2000, p. 197.

[6] - L. Fabbrini, I. Rossetti, L. Forni, Appl. Catal. B: Environm., 44 (2003) 107.

[7] - L. Fabbrini, I. Rossetti, L. Forni, Appl. Catal. B: Environm., 56(3) (2005) 221.

[8] - L. Fabbrini, I. Rossetti, L. Forni, Appl. Catal. B: Environm., submitted.

[9] - W.J. Stark, L. Mädler, S.E. Pratsinis, EP 1,378,489 A1 (2004), to ETH, Zurich.

[10] - K.Y. Jung, Y.C. Kang, Mater. Lett., 58 (2004) 2161.

[11] - S. Kim, J.J. Gislason, R.W. Morton, X.Q. Pan, H.P. Sun, R.M. Laine, Chem. Mater., 16 (2004) 2336.

[12] - T. Johannessen, S. Koutsopoulos, J. Catal., 205 (2002) 404.

[13] - J.M. Mäkelä, H. Keskinen, T. Forsblom, J. Keskiken, J. Mater. Sci.,39 (2004) 2783.

[14] - A. Kilian, T.F. Morse, Aerosol Sci. and Tech., 34 (2001) 227.

[15] - D.J. Seo, S.B. Park, Y.C. Kang, K.L. Choy, J. Nanoparticle Res., 5 (2003) 199.

[16] - G.L. Chiarello, I. Rossetti, L. Forni, J. Catal., 236(2) (2005) 251.

[17] - Selected Powder Diffraction Data, Miner. DBM (1–40), J.C.P.D.S., Swarthmore, PA, 1974–1992.

[18] - L. Mädler, S.E. Pratsinis, J. Am. Ceram. Soc., 85 (7) (2002) 1713.

[19] - W.J. Stark, K. Wegner, S.E. Pratsinis, A. Baiker, J. Catal., 197 (2001) 182.

[20] - E. Campagnoli, A. Tavares, L. Fabbrini, I. Rossetti, Yu.A. Dubitsky, A. Zaopo, L. Forni, Appl. Catal. B: Environm., 55 (2005) 133.

TABLES

Table 1: Measured flame temperature for different fuel mixtures. PA=propionic acid; Xy=Xylene (numbers indicate the volumetric ratio).

	O_2 Δp (bar)	PA	PA/Xy = 8/2	PA/Xy = 2/8
Max flame temperature in the flamelets zone [°C]	1.5	1320	1539	1385
	0.3	1530	1836	2040
Max flame temperature in the main flame zone [°C] (distance from nozzle mouth [cm])	1.5	824 (1.8)	895 (1.1)	1089 (2.5)
	0.3	897 (1.1)	1527 (1.1)	1910 (2.3)

FIGURE CAPTIONS

Fig.1: *A*-*B*): Instantaneous IR images of the flame (fuel: propionic acid) at Δp=1.5 and 0.3 bar, respectively; *C*-*F*): average of six instantaneous images: *C*) propionic acid (Δp=1.5 bar); *D*) Propionic acid/xylene= 8:2 (Δp=1.5 bar); *E*) Propionic acid/xylene= 2/8 (Δp=1.5 bar); *F*) Propionic acid/xylene= 2/8 (Δp=0.3 bar).

Fig.2: SSA *vs*. O_2 discharge velocity.

Fig.3: Effect of xylene addition to propionic acid on the combustion enthalpy per cm^3 of solvent mixture (ΔH_c) and on SSA.

Fig.4: CH_4 conversion *vs*. temperature for catalysts prepared from various solvent mixtures. PA = propionic acid; Xy = xylene (numbers indicate their volumetric ratio).

Fig.5: Durability of samples prepared from various solvent mixtures. PA = propionic acid; Xy = xylene (figures indicate their volumetric ratio). The last three points refer to the residual activity after each of the overheating cycles at 800°C.

Fig.1

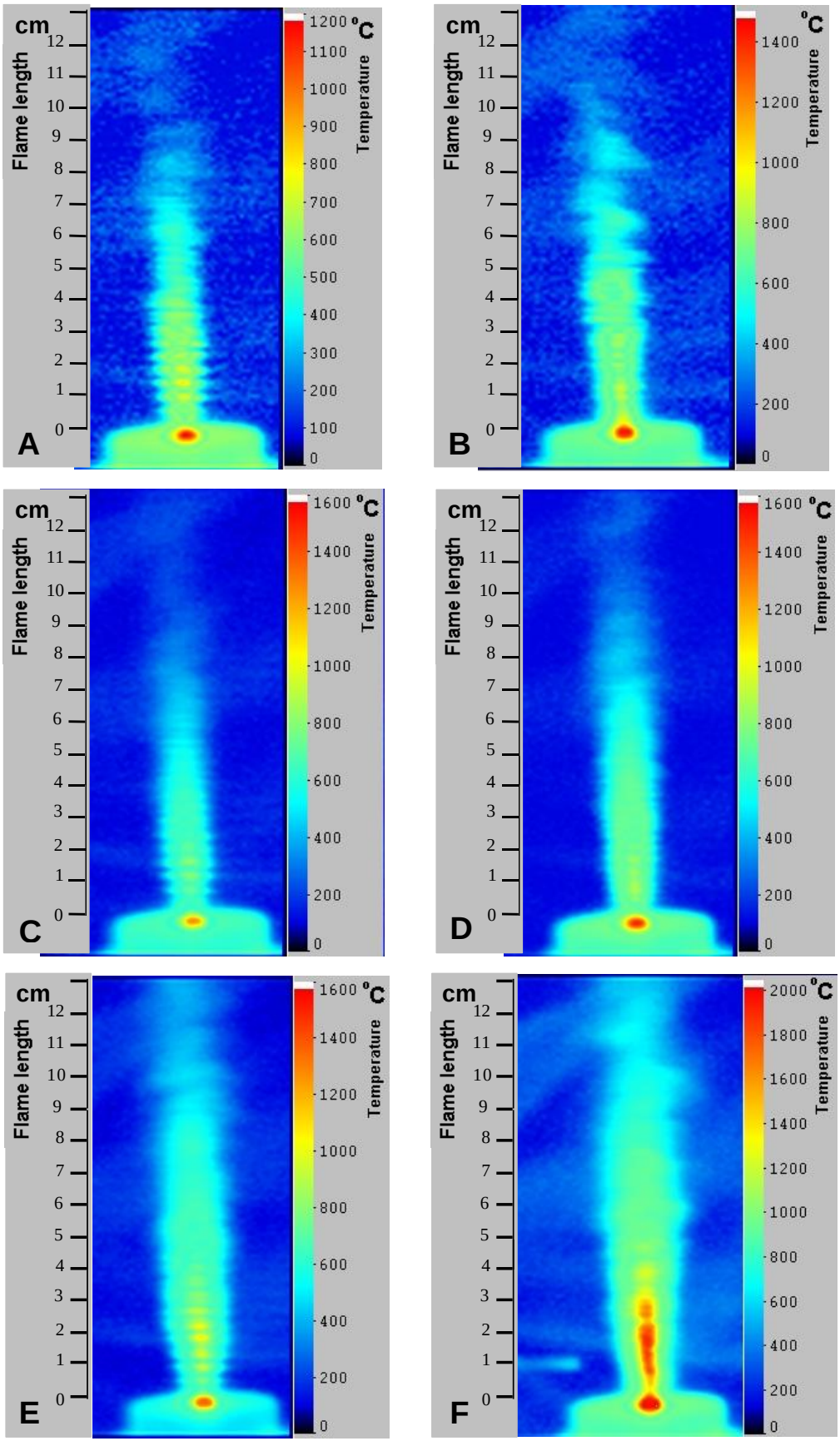
cm
Flame length
12
11
10
9
8
7
6
5
4
3
2
1
0
°C
Temperature
A
1200
1100
1000
900
800
700
600
500
400
300
200
100
0
B
1400
1200
1000
800
600
400
200
0
C
1600
1400
1200
1000
800
600
400
200
0
D
1600
1400
1200
1000
800
600
400
200
0
E
1600
1400
1200
1000
800
600
400
200
0
F
2000
1800
1600
1400
1200
1000
800
600
400
200
0

Fig.2

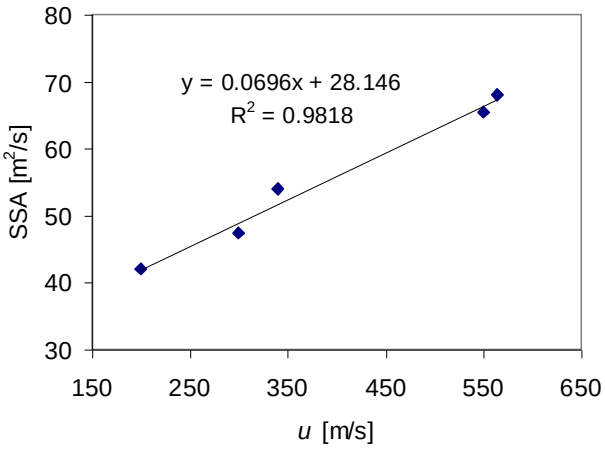
y = 0.0696x + 28.146
R2 = 0.9818
SSA [m2/s]
u [m/s]
80
70
60
50
40
30
150
250
350
450
550
650

Fig.3

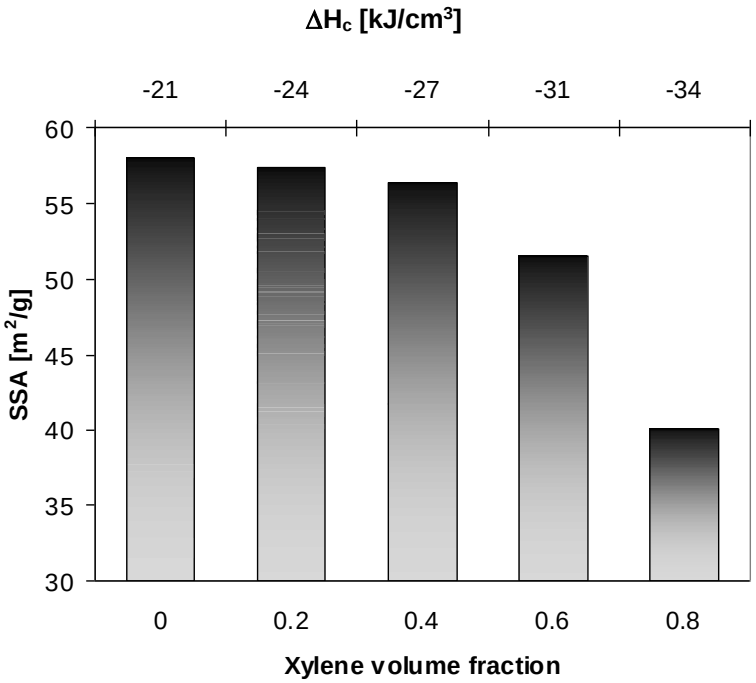
ΔHc [kJ/cm3]
-21
-24
-27
-31
-34
SSA [m2/g]
60
55
50
45
40
35
30
0
0.2
0.4
0.6
0.8
Xylene volume fraction

Fig.4

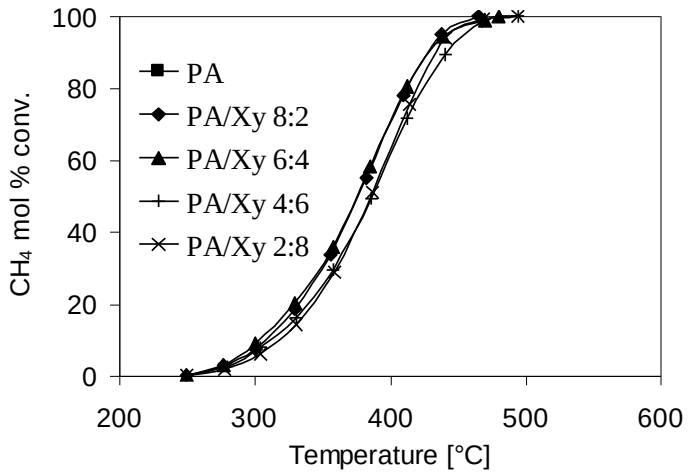
100
80
60
40
20
0
200
300
400
500
600
CH4 mol % conv.
Temperature [°C]
PA
PA/Xy 8:2
PA/Xy 6:4
PA/Xy 4:6
PA/Xy 2:8

Fig.5

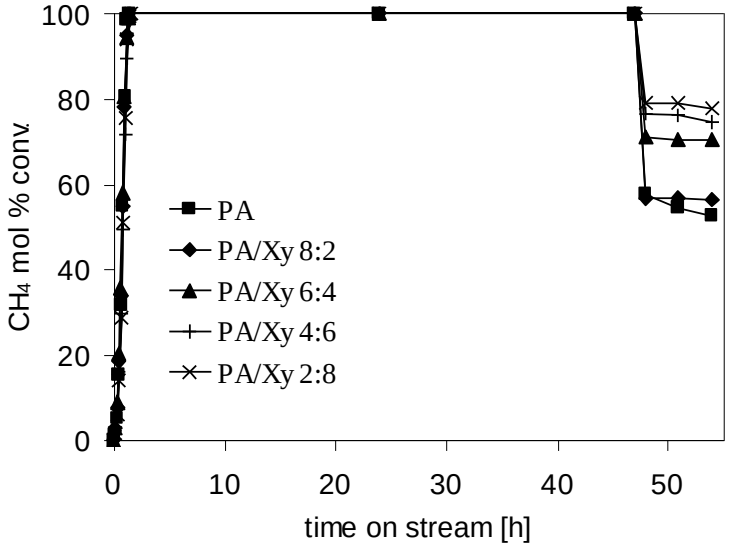
100
80
60
40
20
0
0
10
20
30
40
50
CH4 mol % conv.
time on stream [h]
PA
PA/Xy 8:2
PA/Xy 6:4
PA/Xy 4:6
PA/Xy 2:8